Precambrian Research 170 (2009) 13–26

Contents lists available at ScienceDirect

Precambrian Research

journal homepage: www.elsevier.com/locate/precamres

Paleomagnetism and geochronology of the Malani Igneous Suite, Northwest India: Implications for the configuration of Rodinia and the assembly of Gondwana

Laura C. Gregory[a,*], Joseph G. Meert[a], Bernard Bingen[b], Manoj K. Pandit[c], Trond H. Torsvik[b,d,e]

[a] Department of Geological Sciences, University of Florida, 241 Williamson Hall, Gainesville, FL 32611, United States
[b] Geological Survey of Norway, N-7491, Trondheim, Norway
[c] Department of Geology, University of Rajasthan, Jaipur, 302004, Rajasthan, India
[d] PGP, University of Oslo, 0316 Oslo, Norway
[e] School of Geosciences, Private Bag 3, University of Witwatersrand, WITS2050, South Africa

ARTICLE INFO

Article history:
Received 5 July 2007
Received in revised form 24 October 2008
Accepted 14 November 2008

Keywords:
Rodinia
Malani Igneous Suite
Neoproterozoic
Continental reconstruction, NW India
Paleomagnetism
Geochronology

ABSTRACT

New paleomagnetic and geochronologic data from the Malani Igneous Suite (MIS) in Rajasthan, northwest India, improve the paleogeographic reconstruction of the Indian subcontinent between dispersal of the Mesoproterozoic supercontinent Rodinia and late Neoproterozoic assembly of Gondwana. The MIS comprises voluminous phases of felsic and volumetrically insignificant mafic volcanism followed by granitic plutonism. Large (up to 5 m wide) felsic and mafic dikes represent the terminal phase of magmatism. A zircon U–Pb age on a rhyolitic tuff constrains the initial volcanism in the MIS to 771 ± 5 Ma. A paleomagnetic direction obtained from four mafic dikes has a declination = 358.8° and inclination = 63.5° (with κ = 91.2 and α_{95} = 9.7). It overlaps with previously reported results from felsic MIS rocks. This direction includes a fine-grained mafic dikelet that showed a reversed direction with declination = 195.3° and inclination = −59.7° (κ = 234.8 and α_{95} = 8.1°) and also records an overprint of normal polarity from the larger dikes. The VGP obtained from this study on mafic dikes is combined with previous studies of the Malani suite to obtain a mean paleomagnetic pole of 67.8°N, 72.5°E (A95 = 8.8°). Supported by a tentative baked contact test, we argue that this pole is primary, and permits improved reconstruction of the Indian subcontinent for 771–750 Ma. Data from the MIS and equivalent data from the Seychelles at 750 ± 3 Ma are compared with paleomagnetic data from the 755 ± 3 Ma Mundine Well dikes in Australia to indicate a latitudinal separation of nearly 25° between the Indian and Australian plates. These suggest that East Gondwana was not amalgamated at ca. 750 Ma and therefore these two cratonic blocks were assembled later into the Gondwana supercontinent, during the ca. 550 Ma Kuunga Orogeny.

1. Introduction

The hypothesis of a Meso- to Neo-proterozoic supercontinent amalgamated in the aftermath of Grenvillian orogenesis began to develop in the 1970s (Piper, 1976; Bond et al., 1984). The name of 'Rodinia' was proposed in the early 1990s (McMenamin and McMenamin, 1990; Dalziel, 1991; Moores, 1991; Hoffman, 1991). There are myriad configurations suggested for the Rodinia supercontinent and the exact paleolocations of its constituents are unresolved (Dalziel, 1991; Moores, 1991; Hoffman, 1991; Meert and Torsvik, 2003; Li et al., 2008). The archetypal model for Rodinia outlines that the supercontinent began to form at about 1300 Ma and reached maximum size at about 1000 Ma. Fragmentation and breakup of Rodinia were initiated sometime between 800 and 700 Ma along a rift between western (present-day coordinates) Laurentia and East Antarctica–Australia (Bond et al., 1984; Dalziel, 1991; Hoffman, 1991; Powell et al., 1993). It is hypothesized that this rifting heralded a period of intense global cooling, which stimulated the development of multi-cellular life on Earth (Hoffman et al., 1998; Meert and Lieberman, 2008). Knowledge of the distribution and geotectonic evolution of continents related to Rodinia breakup is critical for an improved understanding of the context and causes of extreme climatic changes and accelerated biologic evolution at the enigmatic boundary between the Neoproterozoic and the Paleozoic.

The assembly of the supercontinent Gondwana followed the fragmentation of Rodinia. Eastern Gondwana comprised cratonic blocks that are currently within India, Madagascar, Sri Lanka, East Antarctica, Australia and the Seychelles. The paleogeography of these cratons prior to the formation and after breakup of Rodinia

* Corresponding author.
E-mail address: laura.gregory@earth.ox.ac.uk (L.C. Gregory).

0301-9268/$ – see front matter © 2008 Elsevier B.V. All rights reserved.
doi:10.1016/j.precamres.2008.11.004

is not well constrained. Some (Windley et al., 1994; Piper, 2000; Yoshida and Upreti, 2006; Squire et al., 2006; Paulsen et al., 2007) argue that these cratons came together in a single collisional event around or even earlier than 1300 Ma, were fused in that same configuration within Rodinia, and remained so until the breakup of Gondwana in the Mesozoic. More consistent with available geologic, paleomagnetic and geochronologic data are the alternative formation of eastern Gondwana as a polyphase assembly of cratonic nuclei that rifted and separately dispersed from the Rodinia supercontinent (Meert et al., 1995; Meert and Torsvik, 2003; Meert, 2003; Boger et al., 2002; Fitzsimons, 2000; Pisarevsky et al., 2003; Collins and Pisarevsky, 2005). This dispute may ultimately be resolved through the acquisition of high-quality paleomagnetic data coupled to high-resolution geochronologic ages from the various cratons that comprise Gondwana. Unfortunately, many extant studies are incomplete in that they do not incorporate an age with paleoposition and thus do not place strong spatial-temporal constraints on ancient continent localities.

The location of India within Gondwana is critical for evaluating the various tectonic models related both to the assembly of greater Gondwana and models of Rodinia. Greater India is placed alongside East Antarctica in the traditional Gondwana fit at 560 Ma (Fig. 1; deWit et al., 1988), and some extrapolate this India–Antarctica–Australia connection to exist within Rodinia and even earlier supercontinents (Dalziel, 1991; Weil et al., 1998; Owada et al., 2003). However, due to paleomagnetic, geochronologic, and geologic correlations (or lack thereof), many workers have since suggested that India maintained a significant latitudinal offset from the archetypal Gondwana fit with Antarctica (Fitzsimons, 2000; Torsvik et al., 2001a; Powell and Pisarevsky, 2002).

The Malani Igneous Suite (MIS) in northwest India provides potentially critical paleomagnetic and geochronologic data for the Indian subcontinent during the late Neoproterozoic. Outcropping in southwest Rajasthan (Fig. 2), the MIS is estimated to be one of the largest felsic igneous suites in the world (>51,000 km^2; Pareek, 1981; Bhushan, 2000). Paleomagnetic studies from the MIS define the key paleomagnetic pole for the Indian subcontinent between 770 and 750 Ma. In this study, we augment previous work via the addition of paleomagnetic data from late-stage mafic dikes along with precise U–Pb ages from earlier erupted rhyolitic tuffs. Combined, these data contribute a key paleopole for the Indian plate during the Neoproterozoic, and lead to a discussion on the drift of India between the breakup of Rodinia and the formation of Gondwana.

2. Geology and tectonic setting

Magmatism in the MIS occurred in three phases (Pareek, 1981). Activity commenced with a volcanic phase made up of predominant felsic and minor mafic flows. The second phase is characterized by the emplacement of granitic plutons. Felsic and mafic dike swarms form the third and final phase of the igneous cycle (Pareek, 1981; Bhushan, 1984; Pandit and Amar Deep, 1997). Malani felsic rocks are un-metamorphosed, but slightly tilted in some areas. Late-stage mafic dikes are all vertical to sub-vertical (Fig. 3a). The MIS unconformably overlies Paleo- to Meso-proterozoic metasediments, and basement granite gneisses and granodiorites of an unknown age (Pandit et al., 1999). The suite is unconformably overlain by the flat-lying late Neoproterozoic to Cambrian Marwar Supergroup, made up of red-bed and evaporite sedimentary sequences (Pandit et al., 2001).

A volcaniclastic conglomerate lies at the base of MIS (Bhushan, 2000) and basal rhyolitic tuffs denote the initiation of the first stage of the suite. Vertical to sub-vertical dolerite dikes crosscut all of the other components and thus mark the termination of magmatism. These mafic dikes are up to 5 m wide (Fig. 3a) and intrude granite within the MIS. The mafic dike sequence near Jalore contains a relatively dense concentration of dikes with a general N–S

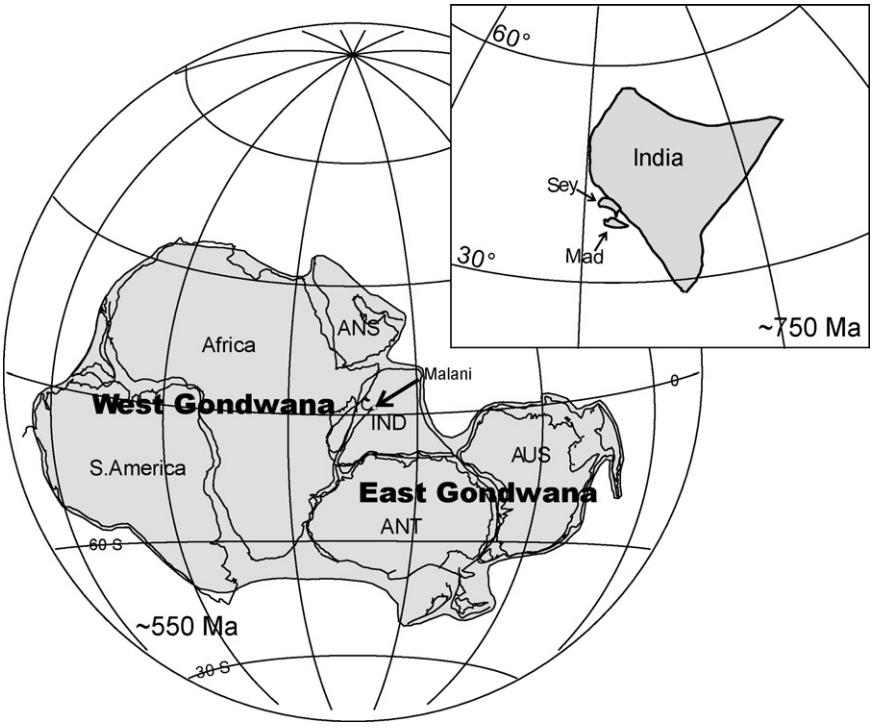

Fig. 1. Traditional Gondwana fit for 560 Ma, taken from deWit et al. (1988). Inset highlights the paleoposition of the Seychelles (Sey) and Madagascar (Mad) relative to India at 750 Ma, reconstructed using the Malani pole (Torsvik et al., 2001a) and the Seychelles Euler pole of rotation (Torsvik et al., 2001b). Euler rotation parameters are Seychelles: 13.3°N, 332.9°E, +48.5°; Madagascar: 20.9°N, 13.8°E, +48.5°.

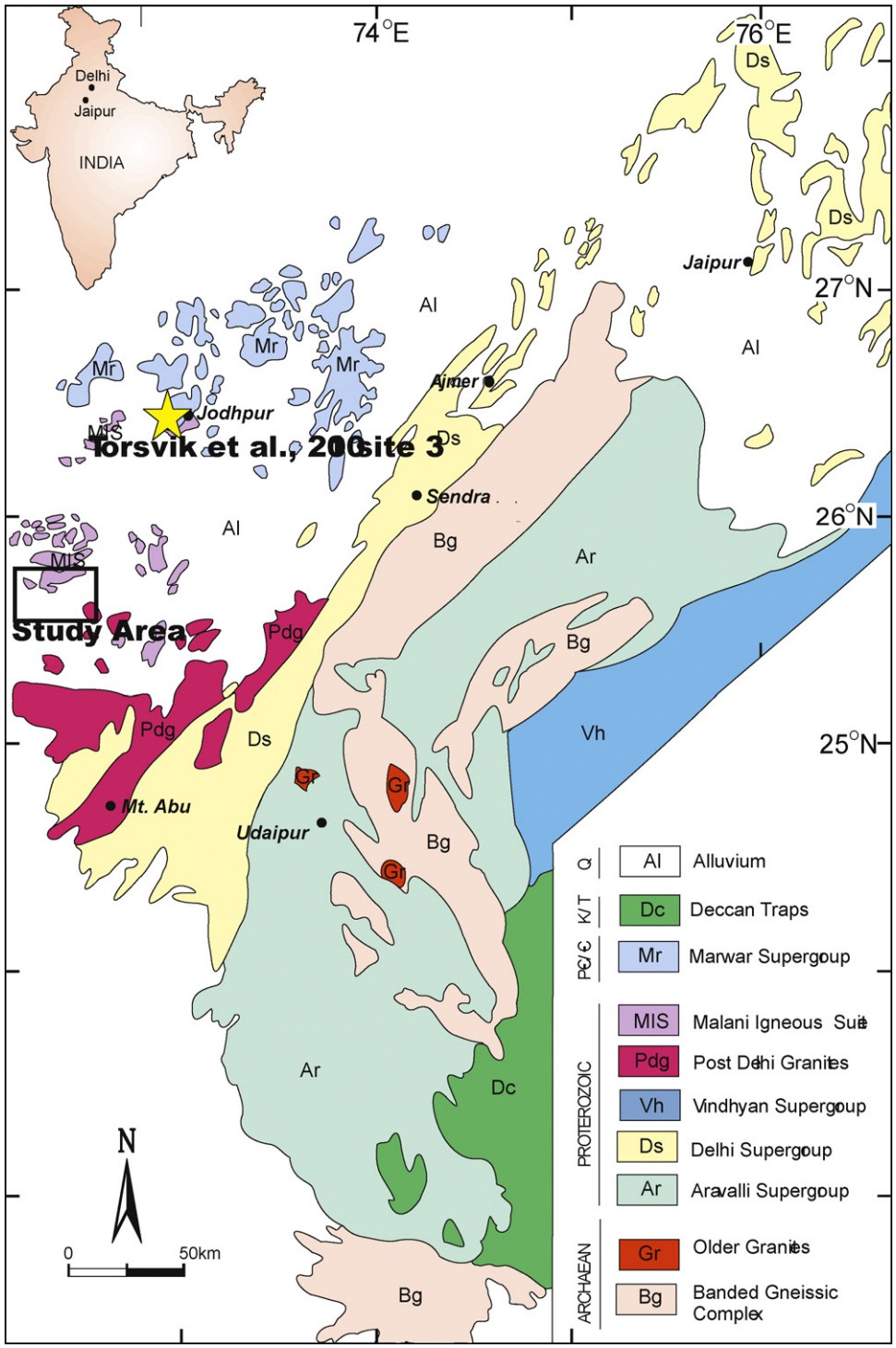

Fig. 2. Map showing Precambrian stratigraphic units of the Aravalli Mountain Region in NW India with sampling area boxed (adapted from GSI publications and other published work).

trend. One large dike trends E–W and likely exploits an existing structural weakness in granite. Many of the larger dikes form conspicuous ridges only when enclosed in a granite host (Fig. 3a) and weather out as bouldery traces visible in satellite images (Fig. 4a).

Neoproterozoic magmatism in NW India can be compared with equivalent Neoproterozoic igneous provinces on nearby cratons. Paleomagnetic data juxtapose the Seychelles alongside India, and northeastern Madagascar is also placed along the India margin based on geochronological and geological similarities (Collins, 2006; Torsvik et al., 2001b; Ashwal et al., 2002). The sequence of rocks on Seychelles is rather similar to the Malani suite, and it is postulated that the geochemical signatures in the Seychelles are sourced from the Archean Banded Gneiss Complex in Rajasthan (Ashwal et al., 2002). The majority of Neoproterozoic granitoid and doleritic activity in the Seychelles falls within 755–748 Ma (Ashwal et al., 2002), with a span of ages ranging from 808 to 703 Ma (Stephens et al., 1997). If the Seychelles suite of Neoproterozoic rocks is analogous to the Malani province, the dolerite dikes sampled in this study can be considered as equivalents to dolerite dikes

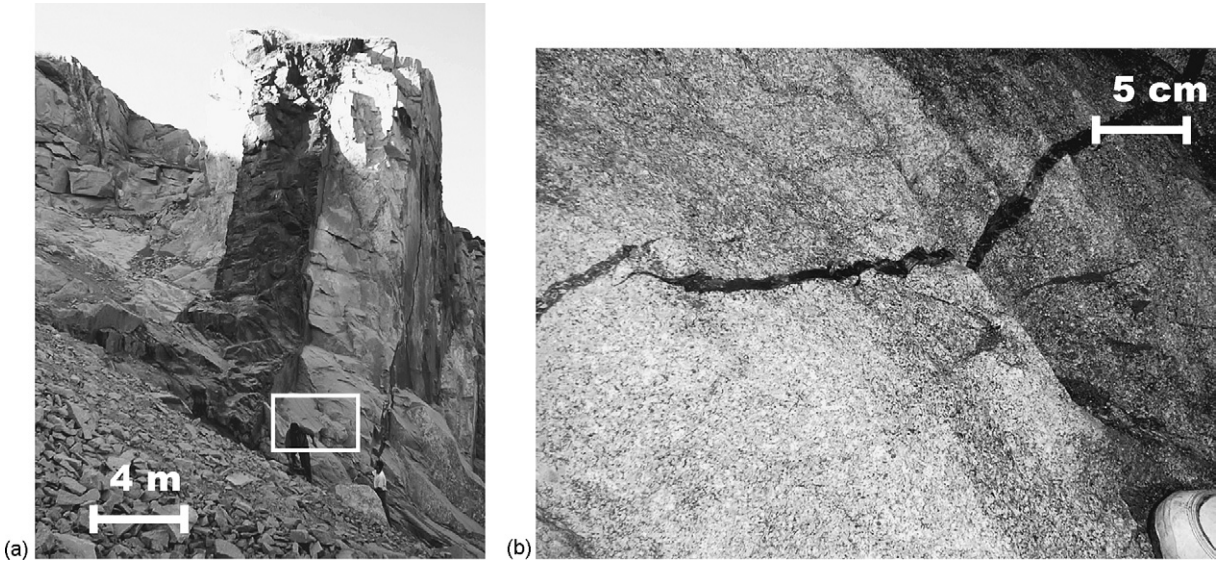

Fig. 3. (a) Photo of a large E–W trending dike in a granite quarry in Jalore (site I434). (b) Photo of 1 cm wide N–S trending mafic dikelet from site I434. Location of (b) is within box in (a).

of Seychelles. The Seychelles dikes are geochemically related to Seychelles granitoids (Ashwal et al., 2002), and a U–Pb zircon age at 750.2 ± 2.5 Ma from one of those dikes (Takamaka dike) indicates that they are nearly coeval with the felsic magmatic suite (Torsvik et al., 2001b). Slightly younger, but overlapping, ages (715–754 Ma) from the Daraina sequence in northern Madagascar are also correlated to the igneous activity in the Seychelles and India (Tucker et al., 1999).

Among the multitude of tectonic settings proposed for Malani magmatism, it is suggested (see Bhushan, 2000) that the first stage of associated basaltic and felsic flows was generated by a hot spot source or lithospheric thinning and melting at the base of the crust due to extension (Sharma, 2004). However, both Madagascar and Seychelles have igneous activity that is attributed to subduction of the Mozambique Ocean (Fig. 1 inset; Handke et al., 1999; Torsvik et al., 2001b; Tucker et al., 2001; Ashwal et al., 2002). This is inter-

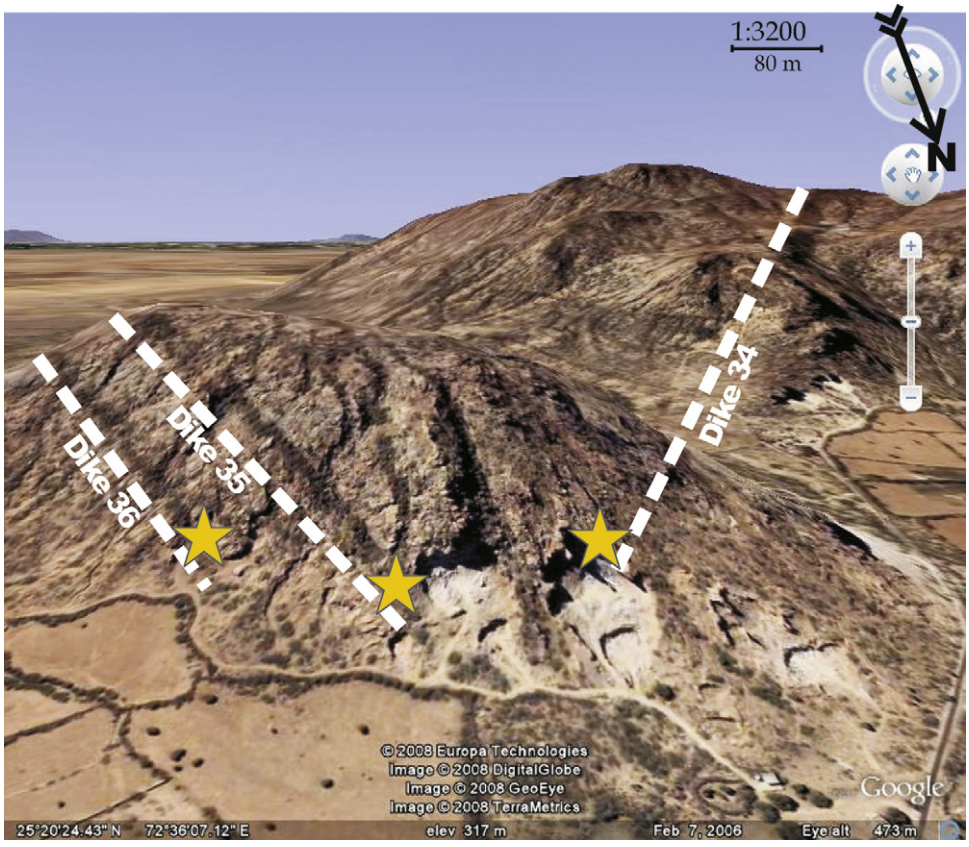

Fig. 4. Google Earth© satellite image of topography and dike traces near Jalore. Azimuths of dike traces are indicated with white lines. Dikes 34, 35, and 36 are the large dikes that were sampled at each respective site. Collection sites are indicated with stars.

preted as an Andean-type active margin, closely related to the nearby and coeval arc activity observed in the Seychelles islands and northeastern Madagascar. The duration of magmatism and the source of igneous activity in the MIS, Seychelles and northeastern Madagascar are still questionable (Collins and Windley, 2002; Collins, 2006).

3. Previous studies

3.1. Paleomagnetism

Numerous paleomagnetic studies have been performed on the felsic members of the MIS to determine the paleoposition of India at ca. 771–750 Ma (Table 1). Athavale et al. (1963) were the first to apply paleomagnetic tests to rhyolitic flows, and their results were similar to those obtained by Klootwijk (1975), but both studies lacked any detailed stability tests. Torsvik et al. (2001a) found a statistically positive fold test on felsic rocks from Malani that constrained the age of magnetism to pre-Marwar age (>Cambrian). Late-stage mafic dikes had not been subjected to paleomagnetic study prior to our work. No reversals or positive field tests were found in previous studies to further document the exact age of magnetism, and this lack of additional positive field tests to fully constrain the age of magnetic acquisition has invoked some doubt in the primary nature of the Malani pole (Yoshida and Upreti, 2006).

3.2. Geochronology

Previous geochronologic results, largely whole-rock Rb–Sr data, from Malani felsic volcanics span about 100 million years (Table 2). Crawford and Compston (1970) reported a Rb–Sr age of 730 ± 10 Ma for rhyolites (re-calculated with a decay constant of 1.42×10^{-11}; see Steiger and Jager, 1977). Dhar et al. (1996) reported a single thermal event at 725 Ma (whole-rock Rb–Sr) for rhyolite and granite emplacement and Rathore et al. (1996, 1999) reported whole-rock Rb–Sr isochron ages ranging from 779 ± 10 to 681 ± 20 Ma for felsic volcanic rocks and granite plutons, emplaced during the first two stages of activity in the MIS (first and second stages, respectively). This wide distribution of dates is partially a result of studies of the so-called ultrapotassic rhyolites found near our sampling locality. The youngest Rb–Sr isochron age of 681 ± 20 Ma (Rathore et al., 1999) resulted from a solitary occurrence of "ultrapotassic" rhyolite, reported without any rock description that would ascertain whether high potassium is a primary igneous character or a later alteration effect. Much younger apparent ages of 548 ± 7–515 ± 6 Ma were obtained from whole-rock $^{40}Ar/^{39}Ar$ data on Jalore granites (Rathore et al., 1999). These apparent ages are interpreted as evidence for a thermal disturbance by Rathore et al. (1999) that may be related to the Kuungan or the Malagasy orogenies (Meert, 2003; Collins and Pisarevsky, 2005); however, the metamorphic grade of MIS rocks is incompatible with any significant thermal resetting (Ashwal et al., 2002). Torsvik et al. (2001a) cited precise U–Pb ages of 771 ± 2 and 751 ± 3 Ma for rhyolite magmatism in the MIS (Tucker, unpublished), but without analytical details and sample descriptions.

4. Methods

4.1. Paleomagnetic sampling and experiments

Samples were obtained in the field using a gasoline powered hand drill and oriented using magnetic and sun compasses. Readings from the sun compass were used to correct for the local declination and any magnetic interference from the outcrop. Twelve samples from Jalore Granite and about 50 samples from four mafic dikes were taken at three sites (Fig. 4). Fresh in-place outcrop is difficult to find and sampling was only possible where the granite host prominently crops out and exposes unweathered dikes. Three samples were taken from a small (width less than 2 cm) fine-grained N–S trending dikelet (Fig. 3b), which is crosscut by a 4-m wide E–W trending mafic dike. This dikelet is aphanitic and dark grey-black in color with chilled margins (Fig. 3b). The dikelet was sampled at less than 1 m away from the larger dike, within a half-dike-width distance, in order to observe the effects of dike emplacement on surrounding rocks. There was no clear generative connection between this small dikelet and larger (nearby) N–S dikes; however, we cannot eliminate the possibility that it is rooted in a larger dike that was not exposed at this particular level in the quarry. It was possible to drill only three cores, as boulders obstructed the remaining dikelet outcrop.

Samples were cut into standard sized specimens and stored in a magnetically shielded space in the University of Florida paleomagnetic laboratory. A few preliminary samples were stepwise treated thermally or with an alternating field to determine the best method of demagnetization. After analyzing the behavior of preliminary samples, a series of steps was chosen for either alternating field or thermal demagnetization. Alternating field demagnetization was applied in steps using an in-house built AF-demagnetizer

Table 1
Summary of Paleomagnetic and Virtual Geomagnetic Poles.

Pole name	Age (Ma)	Pole latitude	Pole longitude	A95 or dp/dm[a]	dec[b]	inc[b]	α_{95}[c]	κ[d]	Reference
India									
Malani, aplite dike	750	74.6N	49.8E	16.2	352.5	60	16.2	18.6	Rao et al., 2003
Malani, rhyolite	745 ± 10	80.5N	43.5E	8/11.5°	354.5	53.5	8		Klootwijk, 1975
Malani, felsic volcanics	751 ± 3, 771 ± 2	74.5N	71.2E	7.4/9.7°	359.5	60.4	6.4	29.9	Torsvik et al., 2001a
Malani, rhyolite	740	78.0N	45.0E	11.0/15.0°	353	56	10		Athavale et al., 1963
Malani, mafic dikes, felsic volcanics	771 ± 5*	70.2N**	70.1E	12.1/15.4°	358.8	63.5	9.7	91.2	This study
Seychelles									
Mahe dikes[IND]	750.2 ± 2.5	79.8N	78.6E	9.9/14.9°	1.4	49.7	11.2		Torsvik et al., 2001b
Australia									
Mundine Well dikes[IND]	755	41.47N	130.92E	4.1/4.1°	14.8	31.1	5		Wingate and Giddings, 2000

[a] A95 = cone of 95% confidence about the mean pole; dp/dm cone of 95% confidence about the paleomagnetic pole in the co-latitude direction (dp) and at a right angle to the co-latitude direction (dm).
[b] dec/inc = mean declination/inclination.
[c] α_{95} = circle of 95% confidence about the mean.
[d] κ = kappa precision parameter.
* U–Pb age data reported in this study, samples are from site 3 of Torsvik et al. (2001a,b).
** Virtual Geomagnetic Pole (VGP) from four dikes.

Table 2
Summary of geochronologic results.

Site	Study	Method	Age (Ma)
Malani			
Rhyolites	Crawford and Compston (1970)	Rb/Sr (recalc with new constant)	730 ± 10
Rhyolites	Klootwijk (1975)	Rb/Sr	745 ± 10
Felsic volcanics	Rathore et al. (1996)	Rb/Sr isochron	779 ± 10
Ultrapotassic rhyolites	Rathore et al. (1999)	Rb/Sr isochron	681 ± 20
Jalore granites	Rathore et al. (1999)	Rb/Sr isochron	727 ± 8
Peralkaline volcanics	Rathore et al. (1999)	Rb/Sr isochron	693 ± 8
Rhyolite	This study, site 3 of Torsvik et al., 2001a	U/Pb	771 ± 5

at fields up to 140 mT. Samples were also treated thermally, in a stepwise manner and up to temperatures of 600 °C for ~60 min using an ASC-Scientific oven. Between each treatment, samples with high magnetic intensity (generally mafic dikes) were measured on a Molspin Magnetometer and samples with low magnetic intensity (dikelets and granites) were measured on a ScT cryogenic magnetometer. Characteristic remanence components (ChRc) were calculated with least-square regression analysis implemented in the Super IAPD program (http://www.ngu.no/geophysics).

4.2. Rock magnetic experiments

The magnetic susceptibility of each sample was measured on an Agico SI-3B bridge before treatment. Curie temperature measurements were carried out on select powdered samples using a KLY-3S susceptibility bridge with a CS-3 heating unit. For this experiment, the susceptibility of a crushed sample is measured at increments during heating and cooling. The character of magnetic minerals in the sample can then be determined in detail based on the change in susceptibility with temperature. Isothermal Remanence Acquisition (IRM) studies were also performed using an ASC-IM30 impulse magnetizer to further characterize magnetic mineralogy.

4.3. Geochronology

Zircon was purified from one sample of rhyolitic tuff using a water table, heavy liquids and a magnetic separator. Available crystals were mounted in epoxy and polished to approximately half thickness. Cathodoluminescence (CL) images were obtained with a scanning electron microscope (Fig. 5). U–Pb analyses were performed by secondary ion mass spectrometry (SIMS) using the CAMECA IMS 1270 instrument at the NORDSIM laboratory, Swedish Museum of Natural History, Stockholm (Table 3). The analytical method, data reduction, error propagation and assessment of the results follow the procedures in Whitehouse et al. (1999). The analyses were conducted with a spot size of ca. 20 μm, calibrating to the Geostandard of 91500-reference zircon with an age of 1065 Ma (Wiedenbeck et al., 1995). The error on the U–Pb ratio includes propagation of the error on the day-to-day calibration curve obtained by regular analysis of the reference zircon. A common Pb correction was applied using the ^{204}Pb concentration and present-day isotopic composition (Stacey and Kramers, 1975). The ISOPLOT program (Ludwig, 1995) was used to regress and present the SIMS U–Pb data.

5. Results

5.1. Geochronologic results

Zircon U–Pb geochronology was conducted on a sample of rhyolitic tuff representing the first stage of volcanism in the MIS. The sample, Mis5/04, was collected close to Jodhpur (26°17.963′–72°58.357′) at site 3 of Torsvik et al. (2001a) where a U–Pb TIMS age of 751 ± 3 Ma was reported as 'personal communication'. The sample shows ca. 5 mm automorphic phenocrysts of quartz, plagioclase and K-feldspar in a microcrystalline devitrified groundmass of rose color. The sample contains few large (ca. 200 μm) prismatic zircon crystals. They show well-terminated pyramid tips and oscillatory zoning and contain common fluid and mineral inclusions. Their habit is typical for zircon formed in a volcanic/subvolcanic magmatic environment. Sixteen analyses were made on 10 zircon crystals. Fourteen of them are concordant and define a concordia age of 771 ± 5 Ma (MSWD = 1.5; Fig. 5). This age is interpreted as the timing of magmatic crystallization and deposition of the rhyolite tuff.

5.2. Rock magnetic results

Mafic dikes have an Isothermal Remanance Magnetization (IRM) plot that is indicative of magnetite (Fig. 6a). Dike samples saturate at ~0.3 T and their remanence intensity remains constant at higher fields, up to the highest applied field of 2 T. Sample I434-28b is a mafic dikelet, and has an IRM curve also characteristic of magnetite, but with a lower absolute J value at saturation (Fig. 6a). In general, Curie temperature runs on samples from the large mafic dikes show a curve that is characteristic of magnetite, but with some alteration upon cooling (Fig. 6b and c). Susceptibility is slightly higher during heating than cooling, but Curie temperatures of all tested dike samples are similar and in the typical range of magnetite. The heating Curie temperature TcH of one dike sample is equal to 589.7 °C and the cooling Curie temperature TcC is equal to 588.3 °C. Fig. 6d and e display Curie temperature results from the small dikelet sam-

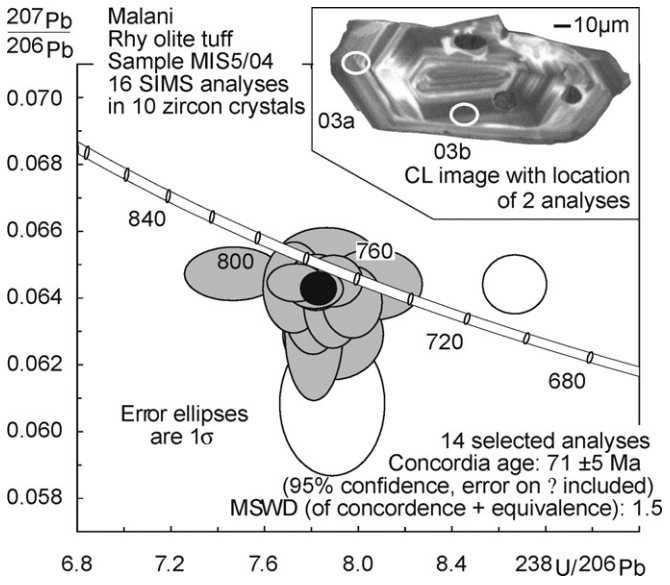

Fig. 5. Inverse concordia diagram showing U–Pb analyses of zircon and CL image of one zircon crystal from a rhyolitic tuff representing the first stage of magmatism in the Malani Igneous Suite. The concordia age of 771 ± 5 Ma reflects magmatic crystallization of the rock.

Table 3
SIMS zircon U–Pb data on rhyolite tuff from Malani Igneous Suite.

ID	U (ppm)	Th (ppm)	Pb (ppm)	$^{206}Pb/^{204}Pb$[a]	$^{207}Pb/^{206}Pb$	±σ (%)	$^{207}Pb/^{235}U$	±σ (%)	$^{206}Pb/^{238}U$	±σ (%)	R[b]	$^{206}Pb/^{238}U$[c] (Ma)	±σ (%)	$^{206}Pb/^{238}U$[d] (Ma)	±σ	Disc.[e] 2σ lim. (%)
MIS5/04: rhyolite tuff[f]																
n1808-01a[g]	222	120	31	10257	0.06439	0.9	1.024	1.4	0.1154	1.0	0.75	704	7	703	7	
n1808-03a	414	202	64	17681	0.06449	0.8	1.127	1.3	0.1267	1.0	0.79	769	8	770	8	
n1808-03b	400	175	62	22494	0.06444	0.6	1.149	1.2	0.1294	1.0	0.87	784	8	785	8	
n1808-04a	85	63	14	5821	0.06372	1.5	1.126	1.8	0.1281	1.0	0.57	777	8	779	8	
n1808-05a	183	106	29	28736	0.06445	0.9	1.137	1.4	0.1279	1.0	0.77	776	8	777	8	
n1808-05b	196	149	33	6602	0.06430	1.4	1.148	1.8	0.1295	1.1	0.62	785	8	786	9	
n1808-05c	55	31	9	3629	0.06296	2.2	1.112	2.4	0.1281	1.0	0.43	777	8	779	8	
n1808-06a	149	113	24	6027	0.06385	1.1	1.104	1.5	0.1254	1.1	0.68	762	8	762	8	
n1808-06b	134	99	22	8903	0.06380	1.4	1.115	1.7	0.1268	1.0	0.60	769	8	771	8	
n1808-07a	401	316	67	13951	0.06426	0.6	1.134	1.2	0.1280	1.0	0.86	777	8	777	8	
n1816-01a	143	101	23	6033	0.06493	1.2	1.139	2.3	0.1272	1.9	0.85	772	14	772	15	
n1816-01b	197	154	32	14111	0.06377	1.0	1.119	2.2	0.1273	2.0	0.89	772	14	773	15	
n1816-02a[g]	46	24	7	3182	0.06076	2.4	1.062	3.0	0.1268	1.9	0.62	770	14	774	14	0.5
n1816-03a	88	57	14	13350	0.06288	1.4	1.099	2.3	0.1268	1.8	0.78	769	13	771	13	
n1816-03b	200	164	35	15016	0.06472	0.8	1.196	2.0	0.1340	1.8	0.91	811	14	812	14	
n1816-06a	138	54	20	10092	0.06440	1.1	1.101	2.0	0.1240	1.7	0.84	754	12	754	12	

[a] Measured $^{206}Pb/^{204}Pb$ ratio.
[b] R, correlation coefficient of errors in isotopic ratios.
[c] ^{204}Pb corrected age.
[d] ^{207}Pb corrected age.
[e] Age discordance at the closest approach of 2σ error ellipse to concordia.
[f] Coordinates of the sample: 26°17.963′–72°58.357′.
[g] Analysis not selected for calculation of concordia age.

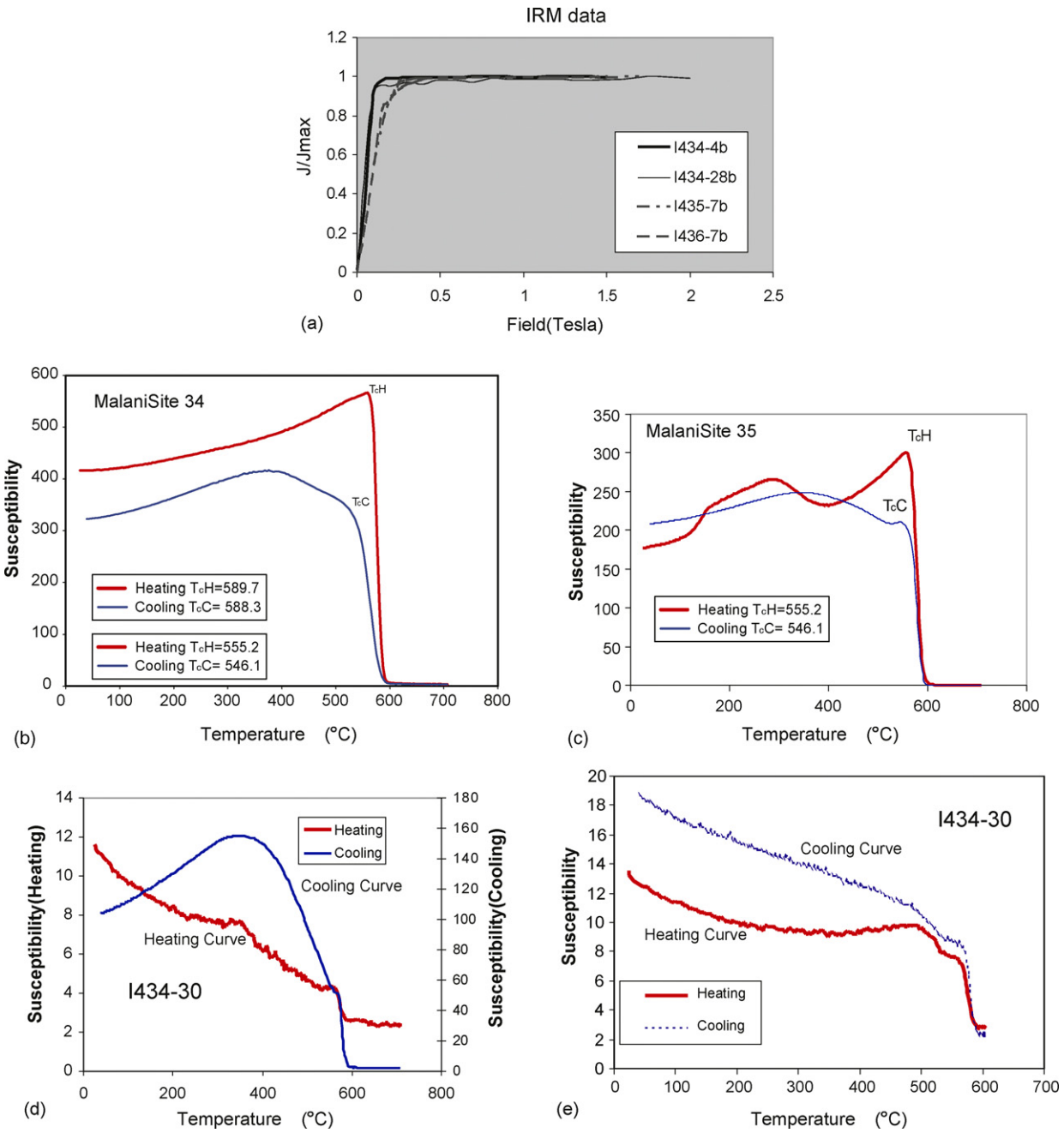

Fig. 6. (a) Isothermal Remanence Magnetization (IRM) plots from four Malani samples. Sample I434-28 is a mafic dikelet. All samples saturate at about 0.3 T. (b) Curie temperature test of typical mafic dike sample from site I434. TcH indicates Curie temperature during heating, and TcC indicates Curie temperature during cooling, (c) Curie temperature test of sample I435-7b – the large mafic dike sampled at site 35. Heating TcH = 555.2 °C, Cooling TcC = 546.1 °C. (d) Curie temperature test of a mafic dikelet heated to 700 °C with significant alteration and high susceptibility during cooling. (e) Curie temperature test of the same mafic dikelet run up to 600 °C, the typical extent of demagnetization temperature. This test shows very little alteration.

pled. When subjected to temperatures up to 700 °C, these mafic dikelets displayed substantial alteration and comparatively high susceptibility while cooling (Fig. 6d). Curie temperature tests were performed on the same samples up to only 600 °C, which is the highest temperature applied during demagnetization. When subjected to the normal range of temperatures, these dikelet samples showed far less alteration (Fig. 6e). We conclude that any alteration observed at lower temperatures is probably due to exsolution and conversion from Ti-magnetite to pure magnetite. Thermal demagnetization curves for large dike samples show unblocking at the characteristic magnetite temperature range of 550–570 °C (Fig. 7a).

In samples from one large dike (at site 36) and the dikelet at site 34 there is evidence for the presence of pyrrhotite, an iron sulfide commonly found in mafic dikes. These samples lose ~40% intensity during thermal demagnetization around 200–250 °C (Fig. 7a), which is within the typical unblocking temperature range for pyrrhotite (Dekkers, 1990). Samples were examined in plain light under microscope, and trace amounts of sulfides were found in samples from site 36 and the dikelet at site 34. We compared low temperature directions (<350 °C) in site 36 to intermediate-high temperature directions (350–580 °C), and found only a few degrees difference (low temperature declination/inclination = 008.2°/+56.5° vs. intermediate tempera-

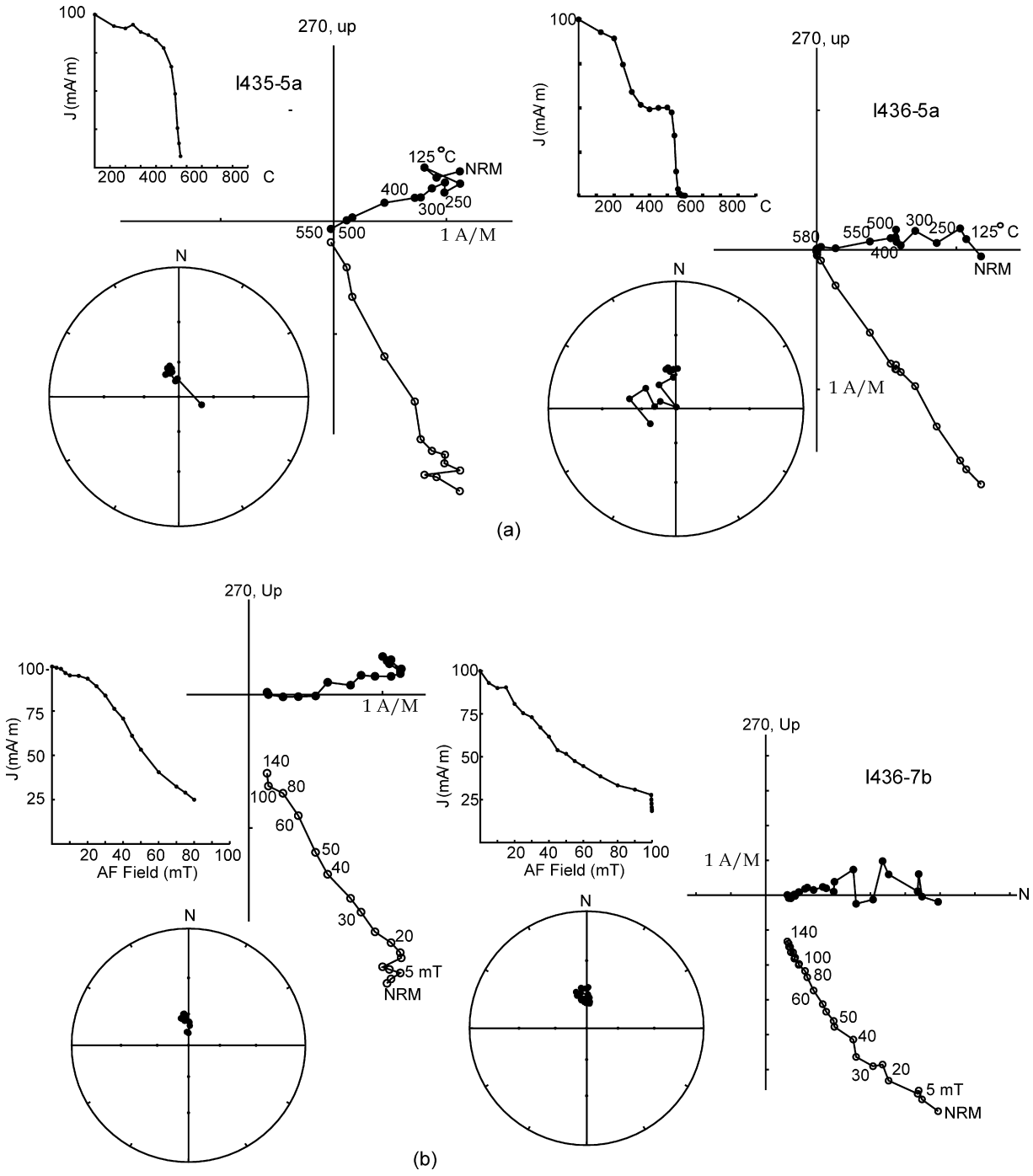

Fig. 7. (a) Thermal and (b) alternating field (AF) demagnetization results of mafic samples from sites 35 and 36. In stereoplots, closed circles represent positive inclinations. In Zijderveld diagrams closed (open) circles represent the horizontal (vertical) plane. NRM = Natural Remanent Magnetization. Thermal measurements are in °C and AF measurements are in millitesla (mT).

ture declination/inclination = 355.4°/+58.2°). This low temperature unblocking direction is either the same as or dominated by the primary magnetization component recognized in intermediate to high temperature demagnetization (>350 °C), and the pyrrhotite effects are likely removed at steps above 350 °C. The directions from samples with pyrrhotite are consistent with samples that do not have any obvious pyrrhotite content, and thus the pyrrhotite was likely formed during deuteric processes and still records a primary direction from the ancient field.

5.3. Paleomagnetic results

Table 4 lists paleomagnetic directions/statistics for each of the dikes in this study. The mean direction resolved from four mafic dikes has a declination = 358.8° and inclination = 63.5° (κ = 91.2 and α_{95} = 9.7), after inverting one reverse polarity dikelet. The overall Virtual Geomagnetic Pole (VGP) calculated from the average direction of each of the four dikes falls at 070.2°N, 70.1°E (dp = 12.1°, dm = 15.4°). Fig. 7 shows the typical demagnetization plots from two mafic dike sites. Most samples show a stable demagnetiza-

Table 4
Paleomagnetic results.

Site name	Latitude/Longitude	n/N[a]	Declination	Inclination	Kappa (κ)[b]	α_{95}[c]	VGP latitude[d]	VGP longitude[d]	dp, dm[e]
This study									
I434 (normal)	25.342°N, 72.601°E	23/27	351.4	72.6	129.55	2.7	56.9N	64.3E	4.3, 4.8
I434 (reverse)	25.342°N, 72.601°E	3/3	195.3	−59.7	234.79	8.1	70.2N	108.8E	9.2, 12.2
I435	25.341°N, 72.601°E	6/8	349.8	61.8	244.78	4.3	70.5N	49.8E	5.1, 6.7
I436	25.341°N, 72.616°E	9/9	355.4	58.2	256.88	3.8	75.9N	57.7E	4.1, 5.6
Combined mean		4 Dikes	358.8	63.5	91.2	9.7	70.2N	70.1E	12.1, 15.4
Torsvik et al. (2001a,b)									
1	26.0°N, 73.0°E	5	038.6	70.6	188.9	5.6	49.7N	106.8E	8.4, 9.7
3	26.3°N, 73.0°E	13	017.2	51.8	678.2	1.6	73.8N	136.7E	1.5, 2.2
4	26.3°N, 72.6°E	13	312.8	72.3	51.7	5.8	44.5N	39.0E	9.1, 10.3
5	26.2°N, 72.5°E	6	356.2	64.1	511.1	3.0	70.1N	64.7E	3.8, 4.8
6	26.4°N, 72.5°E	11	024.7	46.7	178.9	3.4	68.0N	152.8E	2.8, 4.4
8	25.7°N, 72.4°E	16	354.0	59..4	322.0	2.1	74.6N	54.9E	2.4, 3.2
10	25.2°N, 72.6°E	4	339.9	64.0	51.6	12.9	63.9N	39.5E	16.4, 20.5
13	25.6°N, 72.5°E	5	057.5	74.0	109.0	7.3	38.0N	104.7E	11.9 13.2
14	25.7°N, 72.4°E	7	012.7	62.1	200.5	4.3	69.5N	99.6E	5.2, 6.7
Klootwijk (1975)									
RI-2	26.3°N, 73.02°E	6	003.9	62.5	133.0	6.5	72.2N	82.2E	7.9, 10.2
RI-3	26.3°N, 73.02°E	4	023.5	82.5	297.5	5.3	39.6N	80.6E	10.1, 10.3
RI-7	25.8°N, 72.167°E	4	340.0	45.0	55.0	12.5	72.1N	349.0E	10.0, 15.8
RI-10	25.8°N, 72.167°E	5	346.5	52.0	162.0	6.0	76.4N	15.4E	5.6, 8.2
RI-12	25.8°N, 72.167°E	3	337.0	54.5	316.0	7.0	68.2N	12.7E	7.0, 9.9
RI-13	25.67°N, 73.15°E	4	345.0	81.0	490.5	4.0	42.5N	67.1E	7.5, 7.7
Combined mean paleomagnetic pole		19 sites	001.0	63.0	32.9	5.9	67.8N	72.5.E	A95 = 8.8

[a] n = samples used; N = samples collected.
[b] κ = kappa precision parameter.
[c] α_{95} = circle of 95% confidence about the mean.
[d] VGP latitude/longitude = Virtual Geomagnetic Pole.
[e] dp, dm = cone of confidence along site latitude (dp) and orthogonal to site latitude (dm).

tion trend, dependent on the treatment applied. Thermally treated samples unblock between 550 and 570 °C and quickly lose over 50% of their intensity at this temperature range (Fig. 7a). Above 90% loss of initial remanence, samples lose any consistent direction and display random spurious magnetization acquired at high temperatures during demagnetization. Samples treated with an alternating field lose intensity at a more gradual rate and do not generally unblock past greater than 80–85% of the original strength (Fig. 7b). Most samples have a low temperature or low coercivity overprint that has no consistent direction, but is quickly removed. Jalore granite samples were taken with the intent to perform a baked contact test at site 34, but samples are dominated by multi-domain grains that have a strong, but unstable remanence, even with the application of low-temperature liquid nitrogen demagnetization. No stable directions were obtained from any granite samples, and intensity data also have no detectable trend with increasing distance from the large dike (up to 20 m away).

When treated with both alternating field and thermal demagnetization, samples of the fine-grained dikelet at site 34 display a high-temperature component that is antipodal to the three larger Malani dikes (Fig. 8b). Demagnetization trends of the dikelets include two distinct components and samples are weaker in intensity than the larger dikes. They show an increase in intensity at temperatures up to about 490 °C or fields to 40 mT (Fig. 8b). The low temperature and low coercivity component is identical to the mean direction from the normal polarity dikes with a declination = 2.5, inclination = +57.5 (κ = 17.1 and α_{95} = 30.8), which is much steeper than the present-earth field in the region (inclination = 43.4°). The high temperature and high coercivity component has a reverse polarity with declination = 195.3° and inclination = −59.7° (κ = 234.8 and α_{95} = 8.1).

6. Discussion

6.1. Significance of paleomagnetic and geochronologic data

When results from Malani mafic dikes (this study, 4 sites) are combined with the trachyte and rhyolitic volcanics from Torsvik et al. (2001a; 9 sites) and Klootwijk (1975; 6 sites, Table 4), a mean direction is obtained with declination = 001°, inclination = 63.0° (κ = 32.9, α_{95} = 5.9) and paleolatitude of 44.5° . From this mean direction, a paleomagnetic pole for the MIS is placed at 67.8°N, 72.5°E (A95 = 8.8°) after averaging VGPs from the 19 sites. The angular dispersion (S) of measured VGPs can be compared to the latitudinal variation in VGP angular dispersion as determined by Merrill et al. (1996) from IGRF90 (1990 International Geomagnetic Reference Field). VPGs from the Malani suite at paleolatitude 44.5° have an angular variance of 20.7° about the mean pole, calculated from the best estimate of angular variance for VGPs (equation 6.4.2 in Merrill et al., 1996). This value lies within the average VGP scatter for intermediate latitudes that represents the time-averaged field about the earth's spin axis. The mean paleomagnetic pole for the MIS thus sufficiently averages secular variation, and such a scatter is generally inconsistent with a blanket remagnetization of the area.

The focus of this study is to reinforce the mean pole for India at ca. 771–750 Ma with paleomagnetic data from the last stage of MIS magmatism, and pair this with a robust age determination that includes published analytical results. The fortuitous sampling of a small dikelet with unique magnetic behavior provides even further, albeit tentative, support for the primary nature of the Malani pole. No reverse polarity direction or baked contact test was determined in previous work on the Malani suite. There are three possible interpretations for the magnetism observed in the dikelet: (1) the dikelet was emplaced in the same swarm as larger mafic dikes and experienced a true self-reversal, (2) the result is spurious and

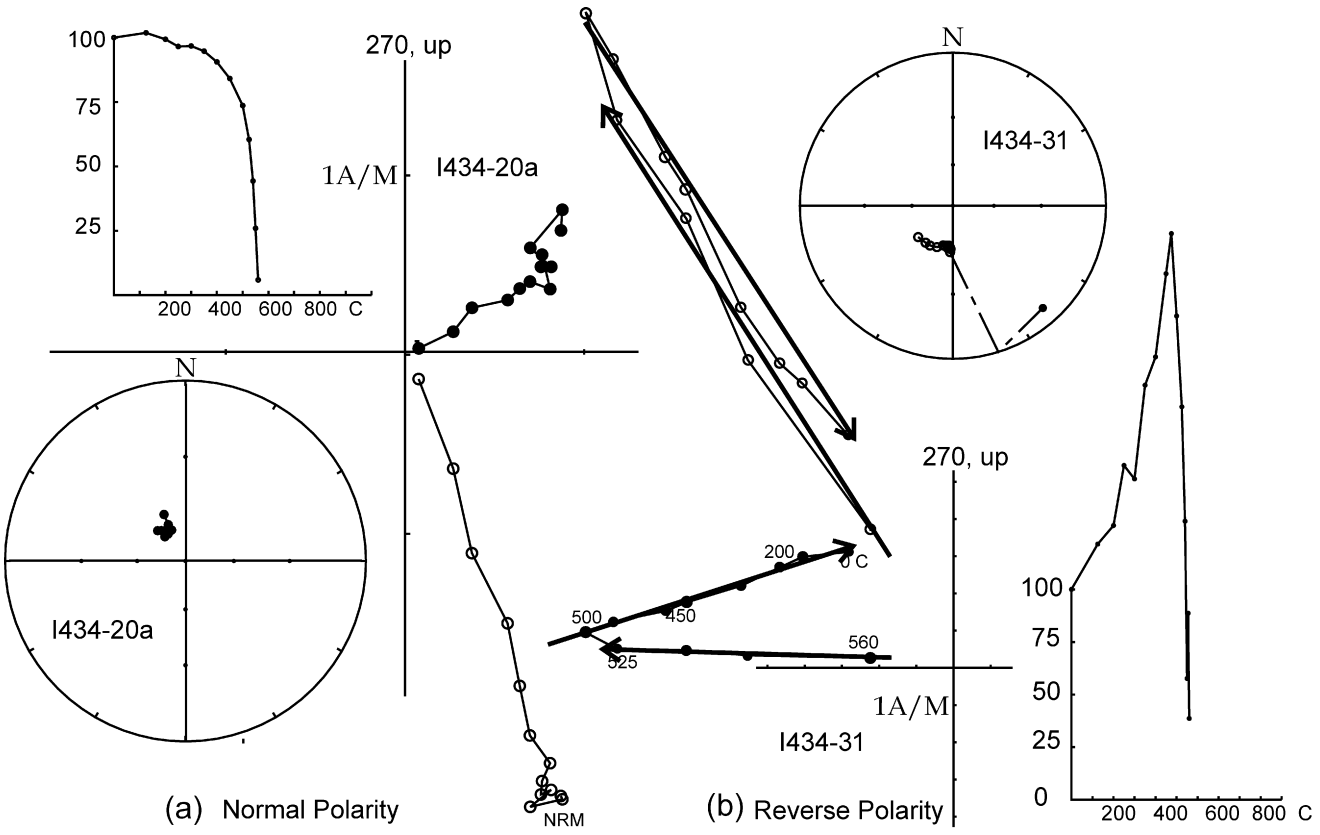

Fig. 8. Demagnetization results from site 34. (a) Normal polarity sample subjected to thermal demagnetization. (b) Reversed polarity dikelet sample with arrows pointing in direction from NRM to origin of both the overprint and reverse polarity vector. In stereoplots, closed circles represent positive inclinations. In Zijderveld diagrams closed (open) circles represent the horizontal (vertical) plane. NRM = Natural Remanent Magnetization. Thermal measurements are in °C and AF measurements are in millitesla (mT).

an unstable anomaly, or (3) the dikelet was emplaced during a main field reversal and baked by the intrusion of subsequent mafic dikes, some time later during a normal polarity field. Option (1) is unlikely based on descriptions of observed natural self-reversing behavior. True self-reversal very rarely occurs in exsolved titanomagnetite compositions of basalt flows. The high Curie temperature phase (magnetite) aligns itself with the external field and influences the low temperature phase to the point of reversal (Merrill and McElhinny, 1983). This occurs in coarse, multi-domain grains during a slower cooling than that associated with aphanitic dikelet emplacement (Petherbridge, 1977; Merrill and McElhinny, 1983). The Malani dikelet has a high temperature direction that is reversed from the rest of the suite, which most likely formed parallel to the external field. This high temperature direction carries the reverse direction, thus even if this is a self-reversal, the reverse polarity direction in the dike is primary and only the low-temperature normal polarity could be an artifact of a true self-reversal. While sampling density is not sufficient to pass statistical reversal tests (i.e. McFadden and McElhinny, 1990), all three samples from the dikelet demonstrated a normal overprint and antipodal directions upon heating.

In our opinion, option (3) best fits the results of the dikelet when compared to the larger dike intrusion. The dikelet was sampled at just within half-dike-width away and thus is still susceptible to partial baking by the large dike. Magnetic intensity increases in all samples as the normal polarity direction is removed (Fig. 8b), which is typical behavior for the demagnetization of magnetic moments that are antipodal to the primary high temperature direction. We suggest that the dikelet was emplaced during a reversed polarity field and was later baked by the adjacent larger dike, resulting in a normal polarity overprint and a reverse primary direction. It is not uncommon for multiple dike intrusions to occur over enough time to include a field reversal. The Harohalli dike swarm in India (Pradhan et al., 2008) and the Matachewan dikes in southern Canada (Irving and Naldrett, 1977; Halls, 1991; Halls and Zhang, 1998; Symons et al., 1994) are examples of dike swarms that were emplaced in multiple phases and include dual-polarity paleomagnetic results.

The Malani pole is cited as a representative pole for India during the late Neoproterozoic, yet some authors conclude that the lack of a decisive reversal or field test deems Malani paleomagnetic data untrustworthy (see Yoshida and Upreti, 2006 for example). However the results of our study not only add to the existing MIS paleomagnetic data set, but also provide additional evidence for a primary magnetization. The fold test yielded by Torsvik et al. (2001a) is now augmented by results that show a primary reverse TRM in the sequence overprinted by a normal-polarity magnetization in the mafic dikelet. Although this does not constitute a 'classic' baked contact test, the result is consistent with baking of the smaller dike by the adjacent E–W trending dike. The Malani pole is distinct from the more common overprints observed in Indian rocks in this region (Deccan and Rajmahal Traps) and from Carboniferous–Cretaceous paleomagnetic results observed in the Gondwana Supergroup and an analysis of post-Cretaceous paleomagnetic poles from India (Mallik et al., 1999; Acton, 1999, Fig. 9). It also does not overlap with the present day field. The positive fold test determined by Torsvik et al. (2001a) constrains the age of the pole to older than Cambrian and ca. 600 Ma paleomagnetic directions from the Indian shield (Halls et al., 2007; Pradhan et al., 2008) show shallow (almost zero inclination), N–S directed magnetizations,

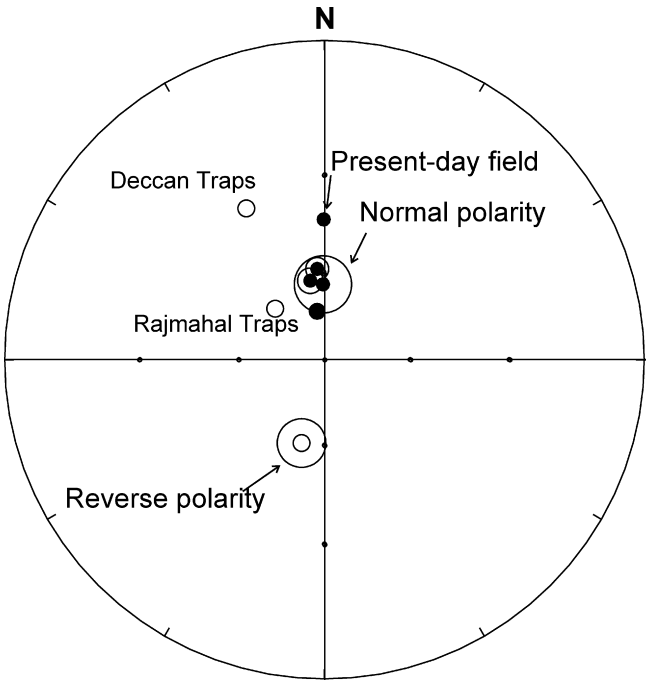

Fig. 9. Stereoplot of individual site means, overall mean and reversed polarity mean with common India overprints from the Deccan Traps and Rajmahal Traps indicated.

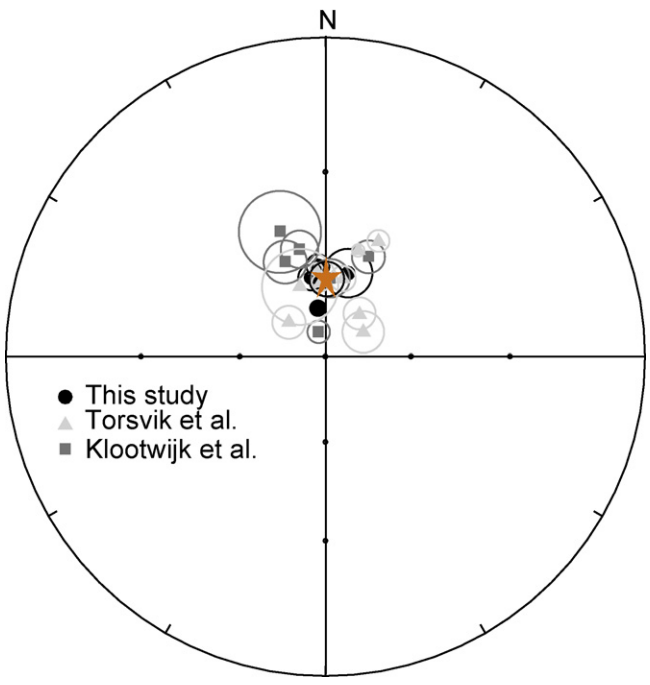

Fig. 10. Stereoplot of directions from three Malani investigations, averaged to the mean pole for the MIS (star). Circles are from mafic dikes (this study); triangles and squares are directions from each site of rhyolite and trachyite volcanics. Closed symbols represent positive inclinations.

distant from the Malani pole. The only potential overprint directions could result from remagnetizations during 600–770 Ma, but no paleomagnetic poles are resolved for India during this time period.

The new zircon extrusion age of 771 ± 5 Ma (Fig. 5) for a rhyolitic tuff places a robust date on the timing of the first stage of magmatism in the MIS. This age is consistent with the first of two 'personal communication' zircon dates at 771 ± 2 and 751 ± 3 Ma quoted by Torsvik et al. (2001a) for rhyolite magmatism in the first stage of MIS magmatism. These ages were determined with TIMS analysis at Washington University, St. Louis, on samples from sites 3 and 4 of Torsvik et al. (2001a), but analytical details were not given in the publication. Available Rb–Sr whole-rock geochronology (Crawford and Compston, 1970; Dhar et al., 1996; Rathore et al., 1999) defines a time span of nearly 100 m.y. (779 ± 10–681 ± 20 Ma), so one cannot rule out that the second and third stages of the magmatism are significantly younger than 771 ± 5 Ma. Nevertheless, the consistency of paleomagnetic data for the different stages of magmatism argues for a comparatively short duration of activity. Paleomagnetic data from Malani dikes overlap with the data from the 750.2 ± 2.5 Ma Takamaka mafic dikes in Seychelles (Torsvik et al., 2001b) providing additional support for the correlation between Malani and Seychelles. In Fig. 10, published site directions determined from the early stage of rhyolitic magmatism in the MIS (Klootwijk, 1975; Torsvik et al., 2001a) are compared to directions derived from the third stage of magmatism of the suite (mafic dikes, this study). The mean direction from all studies is indicated (starred, Fig. 10). We suggest that this indicates a relatively short eruptive history for the Malani suite, contradicting the over 100 million year span of apparent ages derived from Rb–Sr data (Rathore et al., 1999). Younger ages from Rb–Sr data can be accounted for by local disturbances or element mobility during minor episodes of metasomatism. Considering the nature and timing of magmatism in the Seychelles and India, the bulk of granitic and subsequent mafic magmatism in those regions was constrained to the interval from ca. 771 to 751 Ma.

6.2. Implications for the configuration of Rodinia

It is postulated (Powell et al., 1993; Windley et al., 1994; Dalziel, 1997; Yoshida and Upreti, 2006) that a coherent East Gondwana existed from the Mesoproterozoic through the bulk of the Precambrian and until the Mesozoic breakup of Gondwana. This conclusion is largely based on paleomagnetic and detrital zircon data with high flexibility of interpretation and poor age control, as well as the alleged lack of evidence for appropriately aged oceanic sutures between eastern Gondwana cratons. Yoshida and Upreti (2006) discuss evidence for the Neoproterozoic juxtaposition of India and Australia–East Antarctica based on similarities in cratonic and orogenic detrital zircon and neodymium isotopic signatures. Yet the notion of a united East Gondwana through the Proterozoic and Cambrian is contradicted by high-quality paleomagnetic data (Meert and Van der Voo, 1997; Meert, 2001; Torsvik et al., 2001a; Collins and Pisarevsky, 2005). Fitzsimons (2000) and Meert (2003) also review the evidence for appropriately aged mobile belts separating distinct segments of eastern Gondwana elements, which accounts for a later (Cambrian) ocean closure. In their discussion of the proximity of India and Australia–East Antarctica, Yoshida and Upreti (2006) argue that the paleomagnetic data used to constrain the possible separation of these continents do not include a well-constrained age and have been reset by later Pan-African events (~550–510 Ma). We emphasize that this is not a valid argument because both the Malani pole reported in this paper and the highly reliable pole from the 755 ± 3 Ma Mundine Well dike swarm in Australia (Wingate and Giddings, 2000) include necessary field tests to argue against any resetting, and both are well-dated. Furthermore, the Malani pole is quite distinct from ~550 to 510 Ma Gondwana poles (Meert, 2003).

The paleolatitude of the 755 ± 3 Ma Mundine Well dikes is 20.2° and this can be compared to the paleolatitude of the Malani dikes from our study (44.5°), indicating a latitudinal separation of nearly 25° between Australia and India (Fig. 11). If we use the Mundine pole as representative for East Gondwana at 750 Ma, it is necessary

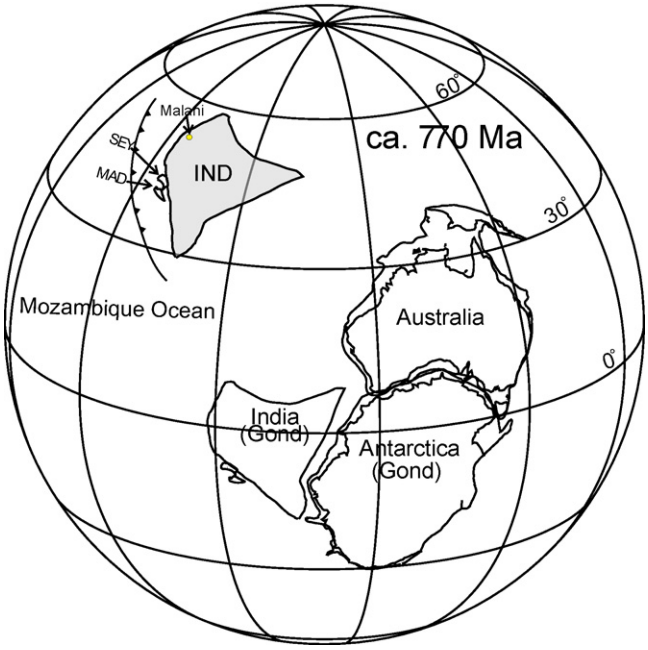

Fig. 11. Reconstruction at 770–750 Ma of pertinent eastern Gondwana components. Grey India outline is plotted from the new mean Malani paleomagnetic pole, with the Seychelles euler rotation fit from Torsvik et al. (2001b) and Madagascar is placed according to the Gondwana fit with India. Australia is plotted according to the Mundine Wells dikes VGP, and Antarctica and India are placed in their Gondwana fit locations, in Australian coordinates. There is >20° of latitudinal displacement between the Malani and Mundine Wells study sites. Euler rotation parameters for the Malani reconstruction are—India: 0°N, 162.5°E, −22.2°; Seychelles: 13.3°N, 332.9°E, +48.5°; Madagascar: 20.9°N, 13.8°E, +48.5°. Euler rotation parameters for the Gondwana fit reconstruction in Australian coordinates are—Australia: 0°N, 45.0°E, +44.0°; Antarctica: 1.6°N, 222.8°E, −75.18°; India: 38.3°N, 141.4°E, +41.1°; Seychelles: 66.7°N, 85.7°E, +38.2°; Madagascar: 22.5°N, 68.5°E, +68.6°.

for the Malani region of India to be located along the paleoequator adjacent to East Antarctica according to its placement in the typically accepted Gondwana fit (deWit et al., 1988). Thus, the misfit between the latitude required by the Malani pole and India's "traditional" position is more than 45°. It is possible that the southeast margin of India was located along the northwestern margin of Australia, but no geologic evidence such as oceanic sutures or similar-aged orogenic belts have been found to support this orientation. Younger-aged sutures between Gondwana components indicate a more complex Gondwana amalgamation as a series of distinct Pan-African orogenies that occurred between ~700 and 500 Ma (Fitzsimons, 2000; Meert, 2003; Collins and Pisarevsky, 2005). The East African Orogen (EAO) is the ~700–650 Ma result of collision between Madagascar, Somalia, Ethiopia and Arabian Nubian shield (collectively Azania block) and the Congo, Tanzania and Bangweulu block, first developed by Stern (1994) and has since been modified (Collins and Pisarevsky, 2005). The later Kuunga Orogen (Meert et al., 1995) places the final Gondwana assembly at about 550 Ma with the amalgamation of Australia–Antarctica with IMSLEK (*I*ndia, northeastern *M*adagascar, *S*ri *L*anka, *E*ast Antarctica, and the *K*alahari craton) group. The Malagasy orogeny is also suggested to occur simultaneously with the Kuunga orogeny as the EAO constituents collided with southeastern India (Collins and Pisarevsky, 2005). These major Pan-African orogenies are congruent with a complex Gondwana assembly.

7. Conclusions

The MIS provides the best paleomagnetic pole for the Indian subcontinent for the time interval from 771 to 750 Ma, with a combined pole of 67.8°N, 72.5°E (A95 = 8.8°). Our study strengthens the case for primary magnetization of the MIS based on the primary reversed direction overprinted by a baked normal-polarity magnetization in a mafic dikelet. The U–Pb zircon age of 771 ± 5 Ma provides an accurate and concordant lower age limit for Malani volcanism. When combined with geochronologic data from mafic dikes in the Seychelles (750.2 ± 2.5, Torsvik et al., 2001b), our age determination also hints at a shorter duration of magmatic activity in the MIS than previously suggested.

East Gondwana is considered by some authors to be a stable configuration from about 1.1 Ga until the Mesozoic breakup of Gondwana (Yoshida and Upreti, 2006). However, paleomagnetic data (Torsvik et al., 2001b, this study) place India and the Seychelles at much higher latitudes than coeval poles from Australia (Mundine dikes, Wingate and Giddings, 2000). Three robust paleomagnetic results (Mundine dykes, Malani Igneous Suite and Takamaka Dikes) are not congruent with an amalgamated East Gondwana at 750 Ma and therefore we argue that the younger Pan-African belts between these cratons resulted from the Neoproterozoic–Cambrian suturing of eastern Gondwana. Thus, if paleomagnetism is to make any contribution to Neoproterozoic plate tectonic models, the Malani pole must be seriously considered in any geodynamic explanation for the assembly of Gondwana.

Acknowledgements

This work was supported by a grant (to JGM) from the National Science Foundation (EAR04-09101). The authors thank Jim Vogl and George Kamenov for help with relentless (unsuccessful) attempts to date the Malani dikes and we also thank Alan Collins and two anonymous reviewers for comments that greatly improved this manuscript. M. Whitehouse is thanked for operating the NORDSIM laboratory and controlling quality of U–Pb data. This is NORDSIM publication 193.

References

Acton, G.D., 1999. Apparent polar wander of India since the Cretaceous with implications for regional tectonics and True Polar Wander. Mem. Geol. Soc. India 44, 129–175.
Ashwal, L.D., Demaiffe, D., Torsvik, T.H., 2002. Petrogenesis of Neoproterozoic granitoids and related rocks from the Seycheeles: evidence for the case of an Andean-type arc origin. J. Petrology 43, 45–83.
Athavale, R.N., Radhakrishnamurthy, C., Sahasrabudhe, P.W., 1963. Paleomagnetism of some Indian rocks. Geophys. J. R. Astronom. Soc. 7, 304–311.
Boger, S.D., Carson, C.J., Fanning, C.M., Hergt, J.M., Wilson, C.J.L., Woodhead, J.D., 2002. Pan-African intraplate deformation in the northern Prince Charles Mountains, east Antarctica. Earth Planet. Sci. Lett. 195, 195–210.
Bond, G.C., Nickeson, P.A., Kominz, M.A., 1984. Breakup of a supercontinent between 625 and 555 Ma: new evidence and implications for continental histories. Earth Planet. Sci. Lett. 70, 325–345.
Bhushan, S.K., 1984. Classification of Malani Igneous Suite. In: Symposium on Three Decades of Developments in Petrology, Mineralogy and Petrochemistry in India, vol. 12. Geol. Surv. India Spec. Publ., pp. 199–205.
Bhushan, S.K., 2000. Malani Rhyolies—A review. Gondwana Res. 3, 65–77.
Collins, A.S., Windley, B.F., 2002. The tectonic evolution of central and northern Madagascar and its place in the final assembly of Gondwana. J. Geol. 110, 325–340.
Collins, A.S., Pisarevsky, S.A., 2005. Amalgamating eastern Gondwana: the evolution of the Circum-Indian Orogens. Earth Sci. Rev. 71, 229–270.
Collins, A.S., 2006. Madagascar and the amalgamation of Central Gondwana. Gondwana Res. (GR Focus) 9, 3–16.
Crawford, A.R., Compston, W., 1970. The age of the Vindhyan system of peninsular India. Quart. J. Geol. Soc. Lond. 125, 351–372.
Dalziel, I.W.D., 1991. Pacific margins of Laurentia and East Antarctica as a conjugate rift pair: evidence and implications for an Eocambrian supercontinent. Geology 19, 598–601.
Dalziel, I.W.D., 1997. Neoproterozoic–Paleozoic geography and tectonics: review, hypothesis and environmental speculation. Bull. Geo. Soc. Am. 109, 16–42.
Dekkers, M.J., 1990. Magnetic monitoring of pyrrhotite alteration during thermal demagnetization. Geophys. Res. Lett. 17, 779–782.
deWit, M.J., Jeffrey, M., Bergh, H., Nicolaysen, L., 1988. Geologic Map of Sectors of Gondwana Reconstructed to their disposition at 150 Ma (1:10,000,000). Am. Assoc. Pet. Geol., Tulsa, OK.

Dhar, S., Frei, R., Kramers, J.D., Nägler, T.F., Kochhar, N., 1996. Sr, Pb and Nd isotope studies and their bearing on the petrogenesis of the Jalore and Siwana complexes, Rajasthan, India. J. Geol. Soc. India 48, 151–160.
Fitzsimons, I.C.W., 2000. A review of tectonic events in the East Antarctic Shield and their implications for Gondwana and earlier supercontinents. J. Afr. Earth Sci. 31, 3–23.
Halls, H.C., 1991. The Matachewan dike swarm, Canada: an early Proterozoic magnetic field reversal. EPSL 105, 279–292.
Halls, H.C., Zhang, B.X., 1998. Uplift structure of the southern Kapuskasing zone from 2.45 Ga dike swarm displacement. Geology 26, 67–70.
Halls, H.C., Jumar, A., Srinavasan, R., Hamilton, M.A., 2007. Paleomagnetism and U-Pb geochronology of easterly geochronology of easterly trending dykes in the Dharwar craton, India: evidence from feldspar clouding, radiating dyke swarms and the position of India at 2.37 Ga. Precam. Res. 151, 47–68.
Handke, M.J., Tucker, R.D., Ashwal, L.D., 1999. Neoproterozoic continental arc magmatism in west-central Madagascar. Geology 27, 351–354.
Hoffman, P.F., Kaufman, A.J., Galen, P.H., Schrag, D.P., 1998. A Neoproterozoic Snowball Earth. Science, New Series 281, 1342–1346.
Hoffman, P.F., 1991. Did the breakout of Laurentia turn Gondwanaland inside out? Science 252, 1409–1412.
Irving, E., Naldrett, A.J., 1977. Paleomagnetism in Abitibi Greenstone Belt and Abitibi and Matachewan diabase dikes: evidence of the Archean geomagnetic field. J. Geol. 85, 157–176.
Klootwijk, C.T., 1975. A note on the Palaeomagnetism of the Late Precambrian Malani Rhyolites near Jodhpur – India. J. Geophys. 41, 189–200.
Li, X.I., Bogdanova, S.V., Collins, A.S., Davidson, A., De Waele, B., Ernst, R.E., Fitzsimons, I.C.W., Fuck, R.A., Gladkochub, D.P., Jacobs, J., Karlstrom, K.E., Lu, S., Natapov, L.M., Pease, V., Pisarevsky, S.A., Thrane, K., Vernikovsky, V., 2008. Assembly, configuration, and break-up history of Rodinia: a synthesis. Precam. Res. 160, 179–210.
Ludwig, K.R., 1995. Isoplot, version 2.82: a plotting and regression program for Radiogenic isotope data. U.S. Geological Survey, Open-file report 91-445, 45 pp.
Mallik, S.B., Piper, J.D.A., Das, A.K., Bandyopadhyay, G., Sherwood, G.J., 1999. Paleomagnetic and rock magnetic studies in the Gondwana Supergroup (Carboniferous–Cretaceous), NE India. Mem. Geol. Soc. India 44, 87–116.
McFadden, P., McElhinny, M.W., 1990. Classification of the reversal test in paleomagnetism. Geophys. J. Int. 103, 725–729.
McMenamin, M.A.S., McMenamin, D.L.S., 1990. The Emergence of Animals; The Cambrian Breakthrough. Columbia Univ. Press, New York, p. 217.
Meert, J.G., Van der Voo, R., Ayub, S., 1995. Paleomagnetic investigation of the Gagwe lavas and Mbozi complex, Tanzania and the assembly of Gondwana. Precam. Res. 74, 225–244.
Meert, J.G., Van der Voo, R., 1997. The assembly of Gondwana 800–550 Ma. J. Geodyn. 23, 223–235.
Meert, J.G., 2001. Growing Gondwana and rethinking Rodinia. Gondwana Res. 4, 279–288.
Meert, J.G., 2003. A synopsis of events related to the assembly of eastern Gondwana. Tectonophysics 362, 1–40.
Meert, J.G., Torsvik, T.H., 2003. The making and unmaking of a supercontinent: Rodinia revisited. Tectonophysics 375, 261–288.
Meert, J.G., Lieberman, B.S., 2008. The Neoproterozoic assembly of Gondwana and its relationship to the Ediacaran–Cambrian radiation. Gondwana Res. 14, 5–21.
Merrill, R.T., McElhinny, M.W., 1983. The Earth's Magnetic Field: Its History, Origin and Planetary Perspective. Int. Geophys. Series 32, Academic Press, 401 p.
Merrill, R.T., McElhinny, M.W., McFadden, P.L., 1996. The Magnetic Field of the Earth: Paleomagnetism, the Core, and the Deep Mantle. Int. Geophys. Series 63, Academic Press, 531 p.
Moores, E.M., 1991. Southwest U.S.-East Antarctica (SWEAT) connection: a hypothesis. Geology 19, 425–428.
Owada, M., Osanai, Y., Toyoshima, T., Tsunogae, T., Hokada, T., Crowe, W.A., Kagami, H., 2003. Early Proterozoic tectonothermal events in the Napier complex, East Antarctica: implications for the formation of East Gondwana. Gondwana Res. 6, 231–240.
Pandit, M.K., Amar Deep, 1997. Petrogenesis of late Proterozoic Malani Suite of rocks in the northwestern fringe of Indian shield. In: Geology of South Asia—II, Geological Survey of Sri Lanka, Spl. Paper 7, pp. 85–91.
Pandit, M.K., Shekhawat, L.S., Ferreira, V.P., Sial, A.N., Bohra, S.K., 1999. Trondhjemite and Granodiorite assemblages from West of Barmer: probable basement for Malani Magmatism in western India. J. Geo. Soc. India 53, 89–96.
Pandit, M.K., Sial, A.N., Jamrani, S.S., Ferreira, V.P., 2001. Carbon isotopic profiles across the Bilara Group rocks of trans-Aravalli Marwar Supergroup in western India: implications for Neoproterozoic–Cambrian transition. Gondwana Res. 4, 387–394.
Pareek, H.S., 1981. Petrochemistry and petrogenesis of the Malani igneous suite, India: summary. Geol. Soc. Am. Bull. 1 (92), 67–70.
Paulsen, T.S., Encarnaciĩon, J., Grunow, A.M., Watkeys, M., 2007. New age constraints for a short pulse in Ross orogen deformation triggered by East-West Gondwana suturing. Gondwana Res. 12, 417–427.
Petherbridge, J., 1977. A magnetic coupling occurring in partial self-reversal of magnetism and its association with increased magnetic viscosity in basalts. Geophys. J. Roy. Astronom. Soc. 50, 395.
Piper, J.D.A., 1976. Palaeomagnetic evidence for a Proterozoic supercontinent. Philos. Trans. R. Soc. Lond. A280, 469–490.
Piper, J.D.A., 2000. The Neoproterozoic Supercontinent: Rodinia or Palaeopangaea? Earth Planet. Sci. Lett. 176, 131–146.
Pisarevsky, S.A., Wingate, T.D., Powell, C.McA., Johnson, S., Evans, D.A.D., 2003. Models of Rodinia assembly and fragmentation. In: Yoshida, M., Windley, B.F., Dasgupta, S. (Eds.), Proterozoic East Gondwana: Supercontinent Assembly and Breakup, vol. 206. Geological Society, London, pp. 35–55 (Special Publications).
Powell, C.McA., McElhinny, M.W., Meert, J.G., Park, J.K., 1993. Paleomagnetic constraints on timing of the Neoproterozoic breakup of Rodinia and the Cambrian formation of Gondwana. Geology 21, 889–892.
Powell, C.M., Pisarevsky, S.A., 2002. Late Neoproterozoic assembly of East Gondwana. Geology 30, 3–6.
Pradhan, V.R., Pandit, M.K., Meert, J.G., 2008. A cautionary note on the age of the paleomagnetic pole obtained from the Harohalli dyke swarms, Dharwar Croton, Southern India. In: Srivastava, S.K., Sivaji, Ch., Rao, N.V.C. (Eds.), Indian Dykes: Geochemistry, Geophysics and Geochronology. Narosa Publishers, Delhi, p. 638.
Rathore, S.S., Venkatesan, T.R., Srivastava, R.K., 1996. Rb–Sr and Ar–Ar systematics of Malani volcanic rocks of southwest Rajasthan: evidence for a younger post crystalline thermal event. Proc. Indian Acad. Sci. (Earth Planet. Sci) 105, 131–141.
Rathore, S.S., Venkatesan, T.R., Srivastava, R.K., 1999. Rb-Sr isotope dating of neoproterozoic (Malani Group) magmatism from southwest Rajasthan, India: evidence of younger pan African thermal event by ^{40}Ar–^{39}Ar studies. Gondwana Res. 2, 271–281.
Sharma, K.K., 2004. The Neoproterozoic Malani magmatism of the northwestern Indian shield: implications for crust-building processes. Proc. Indian Acad. Sci. (Earth Planet. Sci.) 113, 795–807.
Squire, R.J., Campbell, I.H., Allen, C.M., Wilson, C.J.L., 2006. Did the Transgondwanan Supermountain trigger the explosive radiation of animals on Earth? Earth Planet. Sci. Lett. 250, 116–133.
Stacey, J.S., Kramers, J.D., 1975. Approximation of terrestrial lead isotope evolution by a two-stage model. Earth Planet. Sci. Lett. 26, 207–221.
Steiger, R.N., Jager, E., 1977. Subcommission on Geochronology: convention on the use of decay constants in geo- and cosmochronology. Earth Planet. Sci. Lett. 36, 359–362.
Stephens, W.E., Jemielita, R.A., Davis, D., 1997. Evidence for ca. 750 Ma intraplate extensional tectonics from granite magmatism on the Seychelles: new geochronological data and implications for Rodinia reconstructions and fragmentation. Terra Nova 9, 166.
Stern, R.J., 1994. Arc assembly and continental collision in the Neoproterozoic East African orogen: implications for the consolidation of Gondwanaland. Annu. Rev. Earth Planet. Sci. 22, 225–244.
Symons, D.T.A., Lewchuk, M.T., Dunlop, D.J., Costanzoalvarez, V., Halls, H.C., Bates, M.P., Palmer, H.C., Vandall, T.A., 1994. Synopsis of paleomagnetic studies in the Kapuskasing structural zone. Can. J. Earth Sci. 31, 1206–1217.
Torsvik, T.H., Carter, L.M., Ashwal, L.D., Bhushan, S.K., Pandit, M.K., Jamtveit, B., 2001a. Rodinia refined or obscured: palaeomagnetism of the Malani igneous suite (NW India). Precam. Res. 108, 319–333.
Torsvik, T.H., Ashwal, L.D., Tucker, R.D., Eide, E.A., 2001b. Neoproterozoic geochronology and palaeogeography of the Seychelles microcontinent: the India link. Precam. Res. 110, 47–59.
Tucker, R.D., Ashwal, L.D., Hamilton, M.A., Torsvik, T.H., Carter, L.M., 1999. Neoproterozoic silicic magmatism in northern Madagascar, Seychelles and NW India: clues to neoproterozoic supercontinent formation and dispersal. Geol. Soc. Am. Abst. Prog. 31, A317 (abstract).
Tucker, R.D., Ashwal, L.D., Torsvik, T.H., 2001. U–Pb geochronology of Seychelles granitoids: a Neoproterozoic continental arc fragment. Earth Planet. Sci. Lett. 187, 27–38.
Weil, A.B., Van der Voo, R., MacNiocaill, C., Meert, J.G., 1998. The Proterozoic supercontinent Rodinia: Paleomagnetically derived reconstruction for 1100 to 800 Ma. Earth Planet. Sci. Lett. 154, 13–24.
Whitehouse, M.J., Kamber, B.S., Moorbath, S., 1999. Age significance of U–Th–Pb zircon data from early Archaean rocks of west Greenland—a reassessment based on combined ion-microprobe and imaging studies. Chem. Geol. 160, 201–224.
Wiedenbeck, M., Allé, P., Corfu, F., Griffin, W.L., Meier, M., Oberli, F., Von Quadt, A., Roddick, J.C., Spiegel, W., 1995. Three natural zircon standards for (U-Th)/Pb, Lu–Hf, trace element and REE analyses. Geostandards Newsletter 19, 1–23.
Windley, B.F., Razafiniparany, A., Razakamanana, T., Ackermund, D., 1994. Tectonic framework of the Precambrian of Madagascar and its Gondwana connections: a review and reappraisal. Geol. Rundsch. 83, 642–659.
Wingate, M.T.D., Giddings, J.W., 2000. Age and palaeomagnetism of the Mundine Well dyke swarm, Western Australia: implications for an Australia–Laurentia connection at 550 Ma. Precam. Res. 100, 335–357.
Yoshida, M., Upreti, B.N., 2006. Neoproterozoic India within East Gondwana: Constraints from recent geochronologic data from Himalaya. Gondwana Res. 10, 349–356.